Supplemental Material
A Radiative Transfer Framework for Spatially-Correlated Materials

ADRIAN JARABO, Universidad de Zaragoza – I3A
CARLOS ALIAGA, Universidad de Zaragoza – I3A, and Desilico Labs
DIEGO GUTIERREZ, Universidad de Zaragoza – I3A

This is the supplemental material of the paper *"A Radiative Transfer Framework for Spatially-Correlated Materials"*[Jarabo et al. 2018], published in ACM Transactions on Graphics. It includes:

- **Section S.1** – The derivation of the Generalized Boltzmann Equation (GBE) [Larsen and Vasques 2011].
- **Section S.2** – The derivation of the classic Radiative Transfer Equation (RTE) as a special case of the Generalized Boltzmann Equation (GBE).
- **Section S.3** – The derivation that relates Larsen's GBE [2011] as a special case of our Extended GBE (Section 4).
- **Section S.4** – The derivation of the integro-differential form of our Extended GBE (Section 4).
- **Section S.5** – The derivation taking from Equation (15) to Equation (16) in Section 5.1.
- **Section S.6** – The derivations of the classic exponential extinction as a particular case of our local models in Sections 5.1 and 5.2.
- **Section S.7** – Derivation of sampling procedures for Equation (20).
- **Section S.8** – Additional probability distributions of extinction $p(t)$ used in the paper results (Section 6).
- **Section S.9** –Details on Figure 2, including the capture system, the fitting procedure, and additional images on the captured materials.
- **Section S.10** –Analysis on the effect of introducing the Extended GBE in terms of rendering cost and convergence.
- **Section S.11** – Details on the Monte Carlo simulations on explicit correlated volumes, as well as additional results.
- **Figure S.13** – Additional examples of voxelized cloth complementing Figure 11.

S.1 THE GENERALIZED BOLTZMANN EQUATION

Here we include for completeness the derivations of the Generalized Boltzmann Equation (GBE) by Larsen and Vasques [2007; 2011].

Let us define $N(\mathbf{x}, \omega_o, t)\mathrm{d}V\mathrm{d}\Omega\mathrm{d}t$ $[\mathrm{m}^{-3}\,\mathrm{sr}^{-1}\,\mathrm{m}^{-1}]$ as the number of particles in $\mathrm{d}V\mathrm{d}\Omega\mathrm{d}t$ over $\mathbf{x}$ and ω_o that have traveled a distance t since its last interaction (scattering or emission). By considering the net flux of particles $\Phi(\mathbf{x}, \omega_o, t)$ as the number of particles moving a distance $\mathrm{d}t$ in a differential time dt we get

$$\Phi(\mathbf{x}, \omega_o, t) = \frac{\mathrm{d}t}{\mathrm{d}t}N(\mathbf{x}, \omega_o, t) \qquad [\mathrm{m}^{-2}\,\mathrm{sr}^{-1}\,\mathrm{s}^{-1}\,\mathrm{m}^{-1}]$$
$$= v\,N(\mathbf{x}, \omega_o, t), \qquad (S.1)$$

where $v = \frac{\mathrm{d}t}{\mathrm{d}t}$ $[\mathrm{m\,s}^{-1}]$ is the speed of the particles.

By using the classic conservation equation that relates the sources of gain and loss of particles with the rate of change of particles, we get (we use Arvo's notation [1993]):

$$\frac{\mathrm{d}}{\mathrm{d}t}N(\mathbf{x}, \omega_o, t) = \underbrace{(\mathbf{E}(\mathbf{x}, \omega_o, t) + \mathbf{C}_{\mathrm{in}}(\mathbf{x}, \omega_o, t))}_{\text{gains}}$$
$$- \underbrace{(\mathbf{S}(\mathbf{x}, \omega_o, t) + \mathbf{C}_{\mathrm{ext}}(\mathbf{x}, \omega_o, t))}_{\text{losses}}, \qquad (S.2)$$

with $\mathbf{E}(\mathbf{x}, \omega_o, t)$ and $\mathbf{C}_{\mathrm{in}}(\mathbf{x}, \omega_o, t)$ the gains due to particles emission (source) and inscattering respectively, and $\mathbf{S}(\mathbf{x}, \omega_o, t)$ and $\mathbf{C}_{\mathrm{ext}}(\mathbf{x}, \omega_o, t)$ the losses due to particles leaking (streaming) and extinction due to absorption and outscattering.

In the classic steady-state Bolzmann Equation (and therefore the RTE), it holds that the particles and in equilibrium, and therefore $\frac{\mathrm{d}}{\mathrm{d}t}N(\mathbf{x}, \omega_o, t) = 0$. However, the introduction on the t dependence on $N(\mathbf{x}, \omega_o, t)$ introduces a non-zero particles rate over $(\mathbf{x}, \omega_o, t)$. By using the relationship in Equation (S.1), we can compute the rate of change in the number of particles in $\mathrm{d}V\mathrm{d}\Omega\mathrm{d}t$ around $\mathbf{x}, \omega_o, t$ as

$$\frac{\mathrm{d}}{\mathrm{d}t}N(\mathbf{x}, \omega_o, t)\mathrm{d}V\mathrm{d}\Omega\mathrm{d}t = \frac{\mathrm{d}}{v\mathrm{d}t}v\,N(\mathbf{x}, \omega_o, t)\mathrm{d}V\mathrm{d}\Omega\mathrm{d}t \qquad (S.3)$$
$$= \frac{\mathrm{d}}{\mathrm{d}t}\Phi(\mathbf{x}, \omega_o, t)\mathrm{d}V\mathrm{d}\Omega\mathrm{d}t.$$

Using a similar relationship, we can compute net rate of particles leaking out of $\mathrm{d}V$ around $\mathbf{x}$ in direction ω_o after traveling a distance t as

$$\mathbf{S}(\mathbf{x}, \omega_o, t) = \omega_o \cdot \nabla\Phi(\mathbf{x}, \omega_o, t)\mathrm{d}V\mathrm{d}\Omega\mathrm{d}t. \qquad (S.4)$$

Now, let us define $\Sigma(t)$ $[\mathrm{m}^{-1}]$ as the differential probability of extinction, and $\Sigma(t)\mathrm{d}t$ as the probability of a particle to interact at distance $\mathrm{d}t$ after having traveled a distance t since its last interaction (emission or scattering). With these definitions, we can compute the rate of collision (extinction) as

$$\mathbf{C}_{\mathrm{ext}}(\mathbf{x}, \omega_o, t) = \frac{1}{\mathrm{d}t}\Sigma(t)\mathrm{d}t\,N(\mathbf{x}, \omega_o, t)\mathrm{d}V\mathrm{d}\Omega\mathrm{d}t$$
$$= \frac{\mathrm{d}t}{\mathrm{d}t}\Sigma(t)\,N(\mathbf{x}, \omega_o, t)\mathrm{d}V\mathrm{d}\Omega\mathrm{d}t$$
$$= \Sigma(t)\,\Phi(\mathbf{x}, \omega_o, t)\,\mathrm{d}V\mathrm{d}\Omega\mathrm{d}t. \qquad (S.5)$$

The treatment of inscattering and source terms is slightly more complex, given that they set the *memory* of the particles to $t = 0$. Assuming that scattering and absorbers have the same distribution, and therefore we can formulate the differential probability of scattering as $\Sigma_s(t) = \Lambda\,\Sigma(t)$ $[\mathrm{m}^{-1}]$, with Λ [unitless] the probability of scattering of a particle that has suffered collision (scattering albedo). From Equation (S.5), we can compute the rate of particles colliding

at $\mathbf{x}$ from direction ω_i as

$$C_{ext}(\mathbf{x}, \omega_i) = \int_0^\infty C_{ext}(\mathbf{x}, \omega_i, t) dt \qquad (S.6)$$

$$= \left[\int_0^\infty \Sigma(t) \Phi(\mathbf{x}, \omega_i, t) dt \right] dV d\Omega.$$

Then, by multiplying $C_{ext}(\mathbf{x}, \omega_i)$ by the phase function $f_r(\omega_i, \omega_o)$ [sr^{-1}] and the scattering albedo Λ, and integrating over the sphere Ω we get

$$\left[\Lambda \int_\Omega f_r(\omega_i, \omega_o) C_{ext}(\mathbf{x}, \omega_i) d\omega_i \right] dV d\Omega. \qquad (S.7)$$

Since as particles emerge from a scattering event they reset their value t to $t = 0$, then the path length spectrum of inscattering is a delta function $\delta(t)$. Multiplying Equation (S.7) by $\delta(t) dt$ we get $C_{in}(\mathbf{x}, \omega_o, t)$ as

$$C_{in}(\mathbf{x}, \omega_o, t) = \delta(t) \Lambda \left[\int_\Omega f_r(\omega_i, \omega_o) C_{ext}(\mathbf{x}, \omega_i) d\omega_i \right] dV d\Omega dt. \qquad (S.8)$$

Similarly to scattering, emission also requires to set particles to $t = 0$. Following the same reasoning as before, we define the source term $E(\mathbf{x}, \omega_o, t)$ as:

$$E(\mathbf{x}, \omega_o, t) = \delta(t) q(\mathbf{x}, \omega_o) dV d\Omega dt, \qquad (S.9)$$

where $q(\mathbf{x}, \omega_o) dV d\Omega$ [m^{-3} sr^{-1} s^{-1}] is the rate at which particles are emitted by an internal source in $\mathbf{x}$ in direction ω_o.

Substituting Equations (S.4), (S.5), (S.8), and (S.9) into Equation (S.2), and dividing both sides of the equation by $dV d\Omega dt$ we get the final GBE for generic particles transport proposed by Larsen and Vasques [2011, Eq. (2.3)]

$$\frac{d}{dt}\Phi(\mathbf{x}, \omega_o, t) + \omega_o \cdot \nabla\Phi(\mathbf{x}, \omega_o, t) + \Sigma(t)\Phi(\mathbf{x}, \omega_o, t) =$$

$$\delta(t) \Lambda \int_0^\infty \Sigma(s) \int_\Omega \Phi(\mathbf{x}, \omega_i, s) f_r(\omega_i, \omega_o) d\omega_i ds + \delta(t) q(\mathbf{x}, \omega_o), \qquad (S.10)$$

Equation (S.10) defines models transport for general particles as a function of their flux $\Phi(\mathbf{x}, \omega_o, t)$. Since we are interested on light, we want to express such equation in terms of radiance. We can then set $v = c$, with c the speed of light, and assuming monoenergetic photons with wavelength λ [Hz^{-1}], then we define the radiance at $\mathbf{x}$ from direction ω_o, that has traveled a distance t since its last interaction as

$$L(\mathbf{x}, \omega_o, t) = \frac{hc}{\lambda} N(\mathbf{x}, \omega_o, t) = \frac{h}{\lambda} \Phi(\mathbf{x}, \omega_o, t), \quad \left[\frac{W}{m^2 \, sr \, m} \right] \quad (S.11)$$

with h is Plank's constant. Note that the t-resolved radiance $L(\mathbf{x}, \omega_o, t)$ relates with the classic radiance as:

$$L(\mathbf{x}, \omega_o) = \int_0^\infty L(\mathbf{x}, \omega_o, t) dt. \qquad \left[\frac{W}{m^2 \, sr} \right] \qquad (S.12)$$

Similarly, the source term for light $Q(\mathbf{x}, \omega_o)$ is defined in terms of radiant power, and related with $q(\mathbf{x}, \omega_o)$ as

$$Q(\mathbf{x}, \omega_o) = \frac{h}{\lambda} q(\mathbf{x}, \omega_o). \qquad \left[\frac{W}{m^3 \, sr} \right] \qquad (S.13)$$

Therefore, by multiplying Equation (S.10) by $h\lambda^{-1}$ we get the GBE in terms of radiance as

$$\frac{d}{dt}L(\mathbf{x}, \omega_o, t) + \omega_o \cdot \nabla L(\mathbf{x}, \omega_o, t) + \Sigma(t)L(\mathbf{x}, \omega_o, t) =$$

$$\delta(t) \Lambda \int_0^\infty \Sigma(s) \int_\Omega L(\mathbf{x}, \omega_i, s) f_r(\omega_i, \omega_o) d\omega_i ds + \delta(t) Q(\mathbf{x}, \omega_o). \qquad (S.14)$$

Finally, we can obtain the equivalent delta-less form presented in Equation (5): We first set Equation (S.14) for $t > 0$ as

$$\frac{d}{dt}L(\mathbf{x}, \omega_o, t) + \omega_o \cdot \nabla L(\mathbf{x}, \omega_o, t) + \Sigma(t)L(\mathbf{x}, \omega_o, t) = 0. \qquad (S.15)$$

Then, to define the initial value for $t = 0$ of the ODE defined by Equation (S.15) we operate Equation (S.14) with $\lim_{\epsilon \to 0} \int_{-\epsilon}^\epsilon (\cdot) dt$, and using $L(\mathbf{x}, \omega_o, t) = 0$ for $t < 0$ we define

$$L(\mathbf{x}, \omega_o, 0) = \lim t \to 0^+ = L(\mathbf{x}, \omega_o, 0^+) \qquad (S.16)$$

to obtain

$$L(\mathbf{x}, \omega_o, 0) = \int_0^\infty \Sigma_s(t) \int_\Omega L(\mathbf{x}, \omega_i, t) f_r(\omega_i, \omega_o) d\omega_i dt + Q(\mathbf{x}, \omega_o), \qquad (S.17)$$

which is the second line in Equation (5).

S.2 THE RTE AS A SPECIAL CASE OF THE GBE

Here we will see that the classic RTE is a special case of Larsen's Generalized Boltzmann Equation (GBE) [Larsen 2007; Larsen and Vasques 2011], in which the differential extinction probability $\Sigma(t)$ is independent of t, and therefore a constant defined by the extinction coefficient $\Sigma(t) = \mu$.

Let us use the equivalent delta-based form of Equation (5) shown in Equation (S.14). In the classic RTE, the differential probability of extinction is a constant $\Sigma(t) = \mu$, so that Equation (S.14) becomes

$$\frac{d}{dt}L(\mathbf{x}, \omega_o, t) + \omega_o \cdot \nabla L(\mathbf{x}, \omega_o, t) + \mu L(\mathbf{x}, \omega_o, t) =$$

$$\delta(t) \mu_s \int_0^\infty \int_\Omega L(\mathbf{x}, \omega_i, s) f_r(\omega_i, \omega_o) d\omega_i ds + \delta(t) Q(\mathbf{x}, \omega_o) =$$

$$\delta(t) \mu_s \int_\Omega L(\mathbf{x}, \omega_i) f_r(\omega_i, \omega_o) d\omega_i + \delta(t) Q(\mathbf{x}, \omega_o), \qquad (S.18)$$

where $\mu_s = \Lambda \mu$, $L(\mathbf{x}, \omega_i) = \int_0^\infty L(\mathbf{x}, \omega_i, s) ds$. Then, by operating Equation (S.18) by $\int_{-\epsilon}^\infty (\cdot) dt$ (with $\epsilon \approx 0$; note that we cannot use $\epsilon = 0$ because otherwise the integral of the delta function $\delta(t)$ would be undefined) we get

$$L(\mathbf{x}, \omega_o, -\epsilon) + L(\mathbf{x}, \omega_i, \infty) + \omega_o \cdot \nabla L(\mathbf{x}, \omega_o) + \mu L(\mathbf{x}, \omega_o) =$$

$$\mu_s \int_\Omega L(\mathbf{x}, \omega_i) f_r(\omega_i, \omega_o) d\omega_i + Q(\mathbf{x}, \omega_o). \qquad (S.19)$$

Finally, by using $L(\mathbf{x}, \omega_i, -\epsilon) = L(\mathbf{x}, \omega_i, \infty) = 0$ we get

$$\omega_o \cdot \nabla L(\mathbf{x}, \omega_o) + \mu L(\mathbf{x}, \omega_o) =$$

$$\mu_s \int_\Omega L(\mathbf{x}, \omega_i) f_r(\omega_i, \omega_o) d\omega_i + Q(\mathbf{x}, \omega_o), \qquad (S.20)$$

which is the RTE [Equation (1)].

S.3 FROM OUR EXTENDED GBE TO LARSEN'S GBE

Here we demonstrate that our Extended GBE Section 4 is a generalization of Larsen's GBE [Equation (5)], and how the latter can be obtained from ours.

Our Extended GBE is defined as

$$\frac{d}{dt}L(\mathbf{x}, \omega_o, t) + \omega_o \cdot \nabla L(\mathbf{x}, \omega_o, t) + \Sigma_S(\mathbf{x}, t) L_S(\mathbf{x}, \omega_o, t)$$
$$+ \sum_j \Sigma_{Q_j}(\mathbf{x}, t) L_{Q_j}(\mathbf{x}, \omega_o, t) = 0, \qquad (S.21)$$

$$L_S(\mathbf{x}, \omega_o, 0) = \int_0^\infty \int_\Omega \Big(B_S(\mathbf{x}, \omega_i, \omega_o, t) L_S(\mathbf{x}, \omega_i, t) \qquad (S.22)$$
$$+ \sum_j B_{Q_j}(\mathbf{x}, \omega_i, \omega_o, t) L_{Q_j}(\mathbf{x}, \omega_i, t) \Big) d\omega_i dt,$$

$$L_{Q_j}(\mathbf{x}, \omega_o, 0) = Q_j(\mathbf{x}, \omega_o), \qquad (S.23)$$

where

$$L(\mathbf{x}, \omega_o, t) = L_S(\mathbf{x}, \omega_o, t) + \sum_j L_{Q_j}(\mathbf{x}, \omega_o, t), \qquad (S.24)$$

the differential extinction probabilities for the scattered photons and the (unscattered) photons emitted by light source Q_j are respectively $\Sigma_S(\mathbf{x}, t)$ and $\Sigma_{Q_j}(\mathbf{x}, t)$, the scattering operator for scattered photons is $B_S(\mathbf{x}, \omega_i, \omega_o, t) = \Lambda_S(\mathbf{x}, t) \Sigma_S(\mathbf{x}, t) f_{r,S}(\mathbf{x}, \omega_i, \omega_o, t)$, and $B_{Q_j}(\mathbf{x}, \omega_i, \omega_o, t)$ is the scattering operator for photons emitted by light source Q_j.

Equation (S.21) does not impose any assumption on the correlation between scatterers and sources. If they were somehow positively correlated, so that the scatterers and emitters would have the exact same correlation with respect to extincting particles (which could be scatterers or not), then

$$\forall j, \quad \Sigma_S(\mathbf{x}, t) = \Sigma_{Q_j}(\mathbf{x}, t) = \Sigma(\mathbf{x}, t)$$
$$\text{and}$$
$$\forall j, \quad B_S(\mathbf{x}, \omega_i, \omega_o, t) = B_{Q_j}(\mathbf{x}, \omega_i, \omega_o, t) = B(\mathbf{x}, \omega_i, \omega_o, t).$$

This allows us to transform Equation (S.21) into

$$\frac{d}{dt}L(\mathbf{x}, \omega_o, t) + \omega_o \cdot \nabla L(\mathbf{x}, \omega_o, t)$$
$$+ \Sigma(\mathbf{x}, t)\Big(L_S(\mathbf{x}, \omega_o, t) + \sum_j L_{Q_j}(\mathbf{x}, \omega_o, t)\Big) =$$
$$\frac{d}{dt}L(\mathbf{x}, \omega_o, t) + \omega_o \cdot \nabla L(\mathbf{x}, \omega_o, t) + \Sigma(\mathbf{x}, t)L(\mathbf{x}, \omega_o, t) = 0, \quad (S.25)$$

while Equations (S.22) and (S.23) become

$$L_S(\mathbf{x}, \omega_o, 0) = \int_0^\infty \int_\Omega B(\mathbf{x}, \omega_i, \omega_o, t) \Big(L_S(\mathbf{x}, \omega_i, t) \qquad (S.26)$$
$$+ \sum_j L_{Q_j}(\mathbf{x}, \omega_i, t) \Big) d\omega_i dt$$
$$= \int_0^\infty \int_\Omega B(\mathbf{x}, \omega_i, \omega_o, t) L(\mathbf{x}, \omega_o, t) d\omega_i dt,$$
$$L_{Q_j}(\mathbf{x}, \omega_o, 0) = Q_j(\mathbf{x}, \omega_o). \qquad (S.27)$$

From Equations (S.24), (S.26), and (S.27) we can simplify the initial value of Equation (S.25) as:

$$L(\mathbf{x}, \omega_o, 0) = \int_0^\infty \int_\Omega L(\mathbf{x}, \omega_i, t) B(\mathbf{x}, \omega_i, \omega_o, t) d\omega_i dt + Q(\mathbf{x}, \omega_o). \qquad (S.28)$$

Finally, by removing the spatial dependence on $\Sigma(t)$ and the t-dependence on albedo and phase function from Equations (S.25) and (S.28) we get Larsen's GBE [Equation (5)].

S.4 INTEGRAL FORM OF THE EXTENDED GBE

In this section we compute the integro-differential form of our Extended GBE, modeled in differential form in Equations (S.21) to (S.23). Let us first expand Equation (S.21) by using Equation (S.24) as

$$\frac{d}{dt}L_S(\mathbf{x}, \omega_o, t) + \omega_o \cdot \nabla L_S(\mathbf{x}, \omega_o, t) + \Sigma_S(\mathbf{x}, t) L_S(\mathbf{x}, \omega_o, t)$$
$$+ \sum_j \Big(\frac{d}{dt}L_{Q_j}(\mathbf{x}, \omega_o, t) + \omega_o \cdot \nabla L_{Q_j}(\mathbf{x}, \omega_o, t) + \Sigma_{Q_j}(\mathbf{x}, t) L_{Q_j}(\mathbf{x}, \omega_o, t)\Big)$$
$$= 0. \qquad (S.29)$$

This expression is a sum of multiple independent differential equations on $L_S(\mathbf{x}, \omega_o, t)$ and $L_{Q_j}(\mathbf{x}, \omega_o, t)$ with $j \in [1, \infty)$. Since they are independent on each other, we can solve them individually, and them put them back together. Let us first start with the simpler case of L_{Q_j}, by setting $L_S(\mathbf{x}, \omega_o, t) = 0$ and $L_{Q_k} = 0$ for all $k \neq j$, and getting

$$\frac{d}{dt}L_{Q_j}(\mathbf{x}, \omega_o, t) + \omega_o \cdot \nabla L_{Q_j}(\mathbf{x}, \omega_o, t) + \Sigma_{Q_j}(\mathbf{x}, t) L_{Q_j}(\mathbf{x}, \omega_o, t) = 0,$$
$$L_{Q_j}(\mathbf{x}, \omega_o, 0) = Q_j(\mathbf{x}, \omega_o). \qquad (S.30)$$

By solving this partial differential equation we get

$$L_{Q_j}(\mathbf{x}, \omega_o, t) = L_{Q_j}(\mathbf{x}_t, \omega_o, 0) e^{-\int_0^t \Sigma_{Q_j}(\mathbf{x}, s) ds}$$
$$= Q_j(\mathbf{x}, \omega_o) T_{Q_j}(\mathbf{x}, \mathbf{x}_t), \qquad (S.31)$$

where $\mathbf{x}_t = \mathbf{x} - \omega_o t$ and $T_{Q_j}(\mathbf{x}, \mathbf{x}_t) = e^{-\int_0^t \Sigma_{Q_j}(\mathbf{x}, s) ds}$. Then we apply the definite integral on t in the interval $[0, \infty)$ to remove the t dependence as

$$L_{Q_j}(\mathbf{x}, \omega_o) = \int_0^\infty L_{Q_j}(\mathbf{x}, \omega_o, t) dt$$
$$= \int_0^\infty Q_j(\mathbf{x}, \omega_o) T_{Q_j}(\mathbf{x}, \mathbf{x}_t) dt. \qquad (S.32)$$

Now let's consider the case of $L_S(\mathbf{x}, \omega_o, t)$ by setting $L_{Q_k} = 0$ for all k

$$\frac{d}{dt}L_S(\mathbf{x}, \omega_o, t) + \omega_o \cdot \nabla L_S(\mathbf{x}, \omega_o, t) + \Sigma_S(\mathbf{x}, t) L_S(\mathbf{x}, \omega_o, t) = 0,$$
$$L_S(\mathbf{x}, \omega_o, 0) = \int_0^\infty \int_\Omega \Big(B_S(\mathbf{x}, \omega_i, \omega_o, t) L_S(\mathbf{x}, \omega_i, t) \qquad (S.33)$$
$$+ \sum_j B_{Q_j}(\mathbf{x}, \omega_i, \omega_o, t) L_{Q_j}(\mathbf{x}, \omega_i, t) \Big) d\omega_i dt.$$

Again, by solving Equation (S.33), and applying $L_S(\mathbf{x}, \omega_o, 0) = S(\mathbf{x}, \omega_o)$ we get

$$L_S(\mathbf{x}, \omega_o, t) = L_S(\mathbf{x}, \omega_o, 0)\, e^{-\int_0^t \Sigma_S(\mathbf{x}, s)\mathrm{d}s}$$
$$= S(\mathbf{x}, \omega_o)\, T_{L_S}(\mathbf{x}, \mathbf{x}_t). \tag{S.34}$$

which by applying again $\int_0^\infty (\cdot)\mathrm{d}t$ gives

$$L_S j(\mathbf{x}, \omega_o) = \int_0^\infty L_S j(\mathbf{x}, \omega_o, t)\mathrm{d}t$$
$$= \int_0^\infty S(\mathbf{x}, \omega_o)\, T_{L_S}(\mathbf{x}, \mathbf{x}_t)\, \mathrm{d}t. \tag{S.35}$$

Finally, from Equations (S.32) and (S.35) we compute the total radiance $L(\mathbf{x}, \omega_o)$ via Equation (S.24) as

$$L(\mathbf{x}, \omega_o) = \int_0^\infty T_S(\mathbf{x}, \mathbf{x}_t)\, S(\mathbf{x}_t, \omega_o) \tag{S.36}$$
$$+ \sum_j T_{Q_j}(\mathbf{x}, \mathbf{x}_t)\, Q_j(\mathbf{x}_t, \omega_o)\, \mathrm{d}t.$$

S.5 SIMPLIFYING EQUATION (15)

In this section we include the derivations taking from Equation (15) to Equation (16) in Section 5.1 of the main text. Equation (15) computes the transmittance of an incoming beam as

$$T(t) = \int_0^\infty \int_0^\infty p_L(L_i)\, p_\tau(\mu; L_i)\, \frac{L_i}{\hat{L}_i}\, \mathcal{T}(\mu\, t)\, \mathrm{d}\mu\, \mathrm{d}L_i. \tag{S.37}$$

where $p_L(L_i)$ is a probability distribution describing the incoming radiance L_i, $p_\tau(\mu; L_i)$ is the conditional probability distribution describing the distribution of particles as a function of the incoming radiance L_i, and $\hat{L}_i = \int_0^\infty p_L(L_i)\, L_i\, \mathrm{d}L_i$ is the total incoming radiance.

The first assumption we make is that the spatial distributions of incoming light and scatterers are decorrelated. This means that $p_L(L_i)$ and $p_\tau(\mu)$ are independent, so that $p_\tau(\mu; L_i) = p_\tau(\mu)$. This transforms Equation (S.37) into

$$T(t) = \int_0^\infty \int_0^\infty p_L(L_i)\, p_\tau(\mu)\, \frac{L_i}{\hat{L}_i}\, \mathcal{T}(\mu\, t)\, \mathrm{d}\mu\, \mathrm{d}L_i$$
$$= \int_0^\infty p_\tau(\mu)\, \mathcal{T}(\mu\, t) \int_0^\infty p_L(L_i)\, \frac{L_i}{\hat{L}_i}\, \mathrm{d}L_i\, \mathrm{d}\mu$$
$$= \int_0^\infty p_\tau(\mu)\, \mathcal{T}(\mu\, t)\frac{\hat{L}_i}{\hat{L}_i}\mathrm{d}\mu$$
$$= \int_0^\infty p_\tau(\mu)\, \mathcal{T}(\mu\, t)\mathrm{d}\mu. \tag{S.38}$$

Finally, $\mathcal{T}(\mu\, t)$ is the attenuation function, that describes the probability of extinction of an *individual ray*. Note that we have used a generic attenuation function $\mathcal{T}(\tau_t(\mathrm{r}))$; if the particles distribution is random (although correlated) then the extinction at each differential ray of the beam is Poissonian, holding $\mathcal{T}(\tau_t(\mathrm{r})) = e^{-\mu\, t}$. In other cases, in particular in ordered media presenting negative correlation, this attenuation does not hold and extinction becomes a Bernouilli stochastic proccess, which in the limit reduces to a deterministic linear attenuation. By keeping the exponential attenuation,

we transform Equation (S.37) into

$$T(t) = \int_0^\infty p_\tau(\mu)\, e^{-\mu\, t}\mathrm{d}\mu. \tag{S.39}$$

S.6 THE RTE AS A SPECIAL CASE OF OUR LOCAL MODEL

In this section we show how the exponential transmittance predicted by the Beer-Lambert law is a particular case of our model in Section 5.1, in particular how Equation (15), its simplified form [Equation (16)], and the final gamma-based transmittance [Equation (20)] converge to $T(t) = e^{-\overline{\mu}\, t}$, with $\overline{\mu}$ the mean extinction in the differential volume $\mathrm{d}V$.

S.6.1 Equation (15) to exponential transmittance

Starting from Equation (S.37) [Equation (15) in the paper], let us first define the scatterers distribution by setting the probability distribution of extinction $p_\tau(\mu)$. In the classic RTE the assumption is that particles are uniformly distributed in a differential volume, so that the extinction probability is always the same $\overline{\mu}$. Mathematically, this is equivalent to setting

$$p_\tau(\mu) = \delta(\overline{\mu} - \mu), \tag{S.40}$$

where $\delta(s)$ is the Dirac delta function. With that, we can transform Equation (S.37) into

$$T(t) = \int_0^\infty \int_0^\infty p_L(L_i)\, \delta(\overline{\mu} - \mu)\frac{L_i}{\hat{L}_i}\, \mathcal{T}(\mu\, t)\, \mathrm{d}\mu\, \mathrm{d}L_i$$
$$= \int_0^\infty p_L(L_i)\, \frac{L_i}{\hat{L}_i} \int_0^\infty \delta(\overline{\mu} - \mu)\mathcal{T}(\mu\, t)\, \mathrm{d}\mu\, \mathrm{d}L_i$$
$$= \int_0^\infty \frac{L_i}{\hat{L}_i}\mathrm{d}L_i \mathcal{T}(\overline{\mu}\, t)$$
$$= \frac{\hat{L}_i}{\hat{L}_i}\mathcal{T}(\overline{\mu}\, t)$$
$$= \mathcal{T}(\overline{\mu}\, t). \tag{S.41}$$

Finally, we need to define the attenuation process of extinction defined by $\mathcal{T}(\mu\, t)$. Since we are assuming that particles are randomly distributed, then we can safely assume that $\mathcal{T}(\mu\, t)$ is a Poissonian proccess (see Section S.5), where $\mathcal{T}(\mu\, \mathrm{r}) = e^{-\mu\, t}$ holds. By substitution, we therefore transform Equation (S.41) into the exponential transmittance $T(t) = e^{-\overline{\mu}\, t}$. Finally, by applying that $\Sigma(t) = p(t)/T(t)$ we can verify that

$$\Sigma(t) = \frac{p(t)}{T(t)} = \left|\frac{\mathrm{d}T(t)}{\mathrm{d}t}\right|\frac{1}{T(t)} = \frac{\overline{\mu}\, e^{-\overline{\mu}\, t}}{e^{-\overline{\mu}\, t}} = \overline{\mu}, \tag{S.42}$$

which is the t-independent classic form of the differential extinction probability, and which as shown in Section S.2 reduces the GBE to the classic RTE.

S.6.2 Equation (16) to exponential transmittance

Following the same procedure as in the previous section it is easy to verify that by defining a uniform distribution of particles with mean extinction $\overline{\mu}$ via Equation (S.40) we reduce Equation (16) to

the exponential decay as:

$$T(t) = \int_0^\infty p_\tau(\mu) e^{-\mu t} \mathrm{d}\mu$$

$$= \int_0^\infty \delta(\overline{\mu} - \mu) e^{-\mu t} \mathrm{d}\mu$$

$$= e^{-\overline{\mu} t}. \tag{S.43}$$

S.6.3 Equation (20) to exponential transmittance

Finally, we will show that practical gamma-based form of transmittance [Equation (20)], defined as

$$T(t) = \int_0^\infty \Gamma(C; \alpha, \beta) e^{-\mu \sigma t} \mathrm{d}\mu$$

$$= \left(1 + \frac{\overline{\sigma} \cdot t}{\beta}\right)^{-\alpha}, \tag{S.44}$$

with $\Gamma(C; \alpha, \beta)$ the gamma distribution, $\alpha = \overline{C}^2 \cdot \mathrm{Var}(C)^{-1}$, $\beta = \overline{C} \cdot \mathrm{Var}(C)^{-1}$, with $\overline{C}$ and $\mathrm{Var}(C)$ the mean and variance of particles concentration C respectively, and σ the mean cross section. By plugging the definition of α and β in Equation (S.44) we get

$$T(t) = \left(1 + \sigma t \frac{\mathrm{Var}(C)}{\overline{C}}\right)^{-\frac{\overline{C}^2}{\mathrm{Var}(C)}}. \tag{S.45}$$

Then, by applying the limit to Equation (S.46) we get

$$\lim_{\mathrm{Var}(C) \to 0} \left(1 + \sigma t \frac{\mathrm{Var}(C)}{\overline{C}}\right)^{-\frac{\overline{C}^2}{\mathrm{Var}(C)}} = e^{-\overline{C} \sigma t}. \tag{S.46}$$

Finally, by using $\overline{\mu} = \overline{C} \sigma$ we get $T(t) = e^{-\overline{\mu} t}$. A complementary way of formulating this proof is by noticing that $\lim_{\mathrm{Var}(C) \to 0} \Gamma(C; \alpha, \beta) = \delta(\overline{C} - C)$, which results into a very similar derivation to Section S.6.2.

S.7 DERIVATION OF SAMPLING PROCEDURES FOR EQUATION (20)

In Section 5.2 of the main text we define transmittance for distance t in correlated media as [Equation (20)]

$$T(t) = \left(1 + \frac{\overline{\sigma} \cdot t}{\beta}\right)^{-\alpha}, \tag{S.47}$$

with $\alpha = \overline{C}^2 \cdot \mathrm{Var}(C)^{-1}$, $\beta = \overline{C} \cdot \mathrm{Var}(C)^{-1}$, with $\overline{C}$ and $\mathrm{Var}(C)$ the mean and variance of particles concentration C respectively, and σ the mean cross section.

General case $\alpha \in (0, \infty)$
In order to sample a distance t with respect to Equation (20) we need to define the probability function of sampling distance t as $p(t)$. We can compute it using the physical definition of transmittance as:

$$T(t) = \int_t^\infty p(t') \mathrm{d}t', \tag{S.48}$$

from which follows [Equation (21)]

$$p(t) = \left|\frac{\mathrm{d}T(t)}{\mathrm{d}t}\right|$$

$$= \alpha \sigma \frac{\left(\sigma \frac{t}{\beta} + 1\right)^{-(1+\alpha)}}{\beta}, \tag{S.49}$$

which has as CDF

$$P(t) = T(0) - T(t) = 1 - T(t). \tag{S.50}$$

We sample $T(t)$ by using the inverse of Equation (S.50) as

$$t(\xi) = -\frac{\beta}{\sigma} \left(1 - \sqrt[-\alpha]{1 - \xi}\right). \tag{S.51}$$

Sampling Equation (20) **for** $\alpha \in (0, 1)$ Unfortunately, Equation (S.49) is not proportional to Equation (S.48), which is desirable for minimizing variance in Monte Carlo integration. In order to compute such sampling probability we impose $p(t) \propto T(t)$ as $p(t) = C T(t)$, where C is a constant that ensures that $\int_0^\infty p(t') \mathrm{d}t' = 1$. We can thus write

$$C = \frac{1}{\int_0^\infty T(t') \mathrm{d}t'}. \tag{S.52}$$

Solving the integral in the denominator we get

$$\int_0^\infty \left(1 + \frac{\sigma \cdot t'}{\beta}\right)^{-\alpha} \mathrm{d}t' = \frac{(\beta + \sigma t')}{\sigma(1 - \alpha)} \left(1 + \frac{\sigma \cdot t'}{\beta}\right)^{-\alpha}\Bigg|_0^\infty \tag{S.53}$$

$$= -\frac{\beta}{\sigma(1 - \alpha)} + \lim_{t' \to \infty} \frac{(\beta + \sigma t')}{\sigma(1 - \alpha)} \left(1 + \frac{\sigma \cdot t'}{\beta}\right)^{-\alpha},$$

which is convergent for $\alpha > 1$ to

$$\int_0^\infty T(t') \mathrm{d}t' = -\frac{\beta}{\sigma(1 - \alpha)} \tag{S.54}$$

Finally, by using Equations (S.52) and (S.54) we can compute the sampling probability as [Equation (23)]

$$p(t) = -\sigma \frac{1 - \alpha}{\beta}(1 + \frac{\sigma}{\beta}t)^{-\alpha} = -\sigma \frac{1 - \alpha}{\beta} T(t), \tag{S.55}$$

which has CDF

$$P(t) = 1 - (1 + \frac{\sigma}{\beta}t)^{1-\alpha}. \tag{S.56}$$

Finally, we sample Equation (S.55) by inverting Equation (S.56) as [Equation (24)]

$$t(\xi) = P(t)^{-1} = -\frac{\beta}{\sigma} \left(1 - \sqrt[1-\alpha]{1 - \xi}\right). \tag{S.57}$$

S.8 ADDITIONAL PROBABILITY DISTRIBUTIONS OF EXTINCTION

Here we list additional probability distributions of extinction $p(t)$ used in the results of the paper. The first one (Section S.8.1) a perfect negative correlation results into a Bernoulli process (rather than a Poisson process), leading to linear transmittance; the second one (Section S.8.2) models $p(t)$ as a gamma probability distribution. Note that the later is different from our local model in Section 5.2. This second $p(t)$ is important, given that a gamma distribution is in general in good agreement with measured (or computed via Monte Carlo simulations) probability distributions of extinction in particulate materials (see e.g. [Meng et al. 2015, Figure 6]). In the following we list the close-forms of transmittance $T(t)$, probability distribution of extinction $p(t)$, and differential probability of extinction $\Sigma(t)$.

S.8.1 Perfect negative correlation

We define this probability distribution of extinction via the mean extinction coefficient $\bar{\mu}$, as

$$T(t) = \max(0, 1 - \bar{\mu}\, t), \tag{S.58}$$

$$p(t) = \begin{cases} \mu & \text{for } t < \frac{1}{\mu} \\ 0 & \text{elsewhere} \end{cases} \tag{S.59}$$

$$\Sigma(t) = \begin{cases} \frac{\mu}{1-\mu\, t} & \text{for } t < \frac{1}{\mu} \\ 0 & \text{elsewhere} \end{cases}. \tag{S.60}$$

We can sample Equation (S.59) by using

$$t(\xi) = \frac{\xi}{\mu}, \tag{S.61}$$

with $\xi \in (0, 1)$ a uniform random number.

S.8.2 Gamma probability distribution of extinction

In this case, the gamma distribution defines the probability distribution of extinction $p(t) = \Gamma(t; k, \theta)$, parametrized by the parameters $k = \bar{t}^2/\mathrm{Var}(t)$ and $\theta = \mathrm{Var}(t)/\bar{t}$, where $\bar{t}$ is the mean free path, and $\mathrm{Var}(t)$ the variance of the distribution. Note that to avoid confusion with Equation (19) used as $p_C(C)$, we used the alternative parametrization of the gamma distribution, where $k = \alpha$ and $\theta = \beta^{-1}$. This distribution leads to

$$T(t) = 1 - \frac{\gamma_p(k, \theta^{-1}\, t)}{\gamma(k)}, \tag{S.62}$$

$$p(t) = \Gamma(t; k, \theta), \tag{S.63}$$

$$\Sigma(t) = \frac{\Gamma(t; k, \theta)}{1 - \frac{\gamma_p(k, \theta^{-1}\, t)}{\gamma(k)}}, \tag{S.64}$$

where $\gamma_p(s, x) = \int_0^x t^{s-1} e^{-t} \mathrm{d}t$ is the incomplete gamma function, and $\gamma(x)$ is the gamma function. In order to sample Equation (S.63) we do not have a closed form, and need to use numerical methods. In our case, we used the rejection method by Marsaglia and Tsang [2000], which can sample the full space of k, and with cost approximately constant with k.

S.9 DETAILS ON FIGURE 2

In order to validate the existence of non-exponential transmittance, in addition to findings from other fields such as neutron transport or atmospheric sciences, we performed a simple experiment where we capture the transmittance of different correlated (non-exponential) and uncorrelated (exponential) media. For capture, we use a setup inspired in Meng et al. [Meng et al. 2015, Figure 3], where we filled a glass-made vase with the material. The vase was placed on top of a mobile flash for lighting, and captured using a Nikon D200 placed over the vase.

We capture a set of HDR images of increasing thickness for each material. Each image was captured by multi-bracketing 36 RAW images, with fixed aperture set at 4.9, ISO-1600, and exposition time ranging from $1/6400$ s to $1/2$ s. To get rid of the effect of the container we also captured an HDR image of the empty glass. Figures S.1 to S.5 shows the captured materials at different levels of thickness.
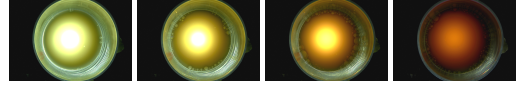
Fig. S.1. Measurements for milk, for thickness from 1 cm to 4 cm.

Fig. S.2. Measurements for black cloth, for increasing number of layers of cloth (from 1 to 4).

Note that the cloth was captured without the glass container. Each material has been tone mapped individually.

Finally, to assess whether the exponential transmittance holds or not on the captured materials, we fit them to an exponential function. As shown in Figure 2, for correlated materials this fitness is not very accurate, while diluted milk shows a very good fit, as expected.

S.10 RENDERING CONVERGENCE

In order to evaluate whether our new model increases variance, we evaluate the convergence of our model with respect to classic exponential transport. We perform this evaluation in the scenes shown in Figures 1 and 17, for three different types of media: classic exponential, and non-exponential with positive and negative correlation. We used volumetric path tracing for rendering. Figure S.6 shows how the error of both media converge in a similar rate with the number of samples (as expected), but that the increment in variance is marginal, and in fact only observable in the case of positive correlation, where the increased transmittance might result in an increase of variance. A similar behavior is observed with the converge with respect to rendering time, since ray-geometry intersections dominate. Figures S.7 and S.8 show a visual comparison of the convergence for each scene.

S.11 MONTE CARLO NUMERICAL SIMULATIONS

In order to gain understanding on the problem, illustrate the results, and compare our solutions against a ground truth, we computed a number of simulations on procedurally generated explicit media. This allowed us to investigate on the differences on the probability distribution of extinction $p(t)$ between scatterers and sources (Section 4), as well to study the effect of boundary conditions (Section 4.3). Here we explain the details of such simulations, including the definitions of the media, and include the full set of results of our simulations.

S.11.1 Modeling correlated scatterers

Since we are interested on the average behavior of $p(t)$, we procedurally generated different types of media in 2D. We opted for a two-dimensional problem since it is simpler but valid to our problem (extinction is a 1D problem), as has been shown in many previous works in transport related fields. Each media was formed by a number of circular scatterers with same (very small) radius r. For each realization of the 2D volume, we build a randomized procedural

Fig. S.3. Measurements for white cloth, for increasing number of layers of cloth (from 1 to 10).

Fig. S.4. Measurements for maldon salt, for thickness from 1 cm to 5 cm.
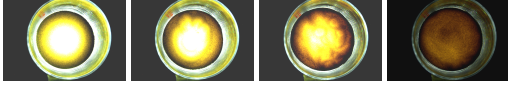
Fig. S.5. Measurements for sugar, for thickness from 1 cm to 4 cm.

media. These procedural definitions were different for the case of positive and negative media.

- **Negatively Correlated Media**: Based on previous work on transport on Lorentz gases [Dumas et al. 1996][1], we generate a perfect negative media by deterministically defining the position of the particles in an array. We introduced the constraint of having each particle in the middle of an hexagon, where the closest neighbor particles where at the vertices of that hexagon. That ensured that the closest particles where all at the same distance. We then slightly displaced each vertex position to ensure that none of them masked any other particle along the propagation direction of the ray. Finally, we stochastically perturbed the position of the particles based on the desired degree of correlation η: We decided whether a particle should be perturbed with probability $p_p = 1 - |\eta|$, and perturbed its position $\mathbf{x}$ as $\mathbf{x} = \mathbf{x}_0 + \omega s$, where $\mathbf{x}_0$ is the particle original position, ω is a unit vector uniformly sampled in the circle of directions, and $s = -\log(\xi)(1-|\eta|)^2$ with ξ a uniform random number.

- **Positively Correlated Media**: Here we follow the approach of Shaw et al. [2002] and Larsen and Clark [2014]: We select the position of a first particle $\mathbf{x}_0$ by uniformly random sampling the unit square. Then, we begin a random walk from this initial position, so that the position $\mathbf{x}_i$ of a particle $i > 0$ is computed as $\mathbf{x}_i = \mathbf{x}_{i-1} + \omega s$, where ω is a unit vector uniformly sampled in the circle of directions, and $s = -\log(\xi)(1-\eta)^2$ with ξ a uniform random number and $\eta \in (0, 1)$ the degree of positive correlation.

In both cases, we use a periodic boundary condition following previous work [Shaw et al. 2002]. Note that we did not impose a minimum distance of particles (that could be another form of negative correlation by using a dart-throwing sampling approach; we did so to avoid introducing some form of correlation when each of the approaches converge to the uncorrelated behavior (i.e. $\eta \to 0$); however, given the small radii of the simulated particles

---

[1]A Lorentz gas is a periodic array of scatterers forming a lattice.

(10^{-5}, distributed in a unit squared medium) we found that they were unlikely to intersect each other.

In the following, we show numerical solutions for source-to-scatterer and scatterer-to-scatterer probability distributions of extinction and transmittance (Section S.11.2), as well as simulations on the medium-to-medium boundary conditions (see Section 4.3) for a variety of different media correlations.

S.11.2 Source-to-Scatterer and Scatterer-to-Scatterer Extinction

Figures S.9 and S.10 show a series transmittances $T(t)$ for a source term at the boundary of the medium, and for scatterer-to-scatterer transport, respectively. Each of them has been computed for a different level of correlation $\eta_1 = \in [-1, 0.9]$. We have simulated each of them by averaging 2000 iterations each iteration with a different randomly generated medium, and 1000 samples per iteration. The samples from the source $Q(\mathbf{x}, \omega_o)$ where traced from the boundary of the medium, for a given direction θ. In contrast, the samples for the scatterer-to-scatterer extinction were traced from the scatterers, by randomly selecting the scatterer of origin, and with a random direction.

S.11.3 Boundary Conditions

Figures S.11 and S.12 shows a wider range of results for the media-to-media boundary, complementing those in Figure 9, for $\eta_1 \in [-1, 0.9]$. We follow the same procedure as in Figure S.9, with a change of media at distance $t = 20$.

REFERENCES

John Amanatides and Andrew Woo. 1987. A fast voxel traversal algorithm for ray tracing. In *Eurographics*, Vol. 87. 3–10.

James Arvo. 1993. Transfer equations in global illumination. *SIGGRAPH '93 Course Notes* 2 (1993).

H. Scott Dumas, Laurent Dumas, and François Golse. 1996. On the mean free path for a periodic array of spherical obstacles. *Journal of statistical physics* 82, 5 (1996), 1385–1407.

Adrian Jarabo, Carlos Aliaga, and Diego Gutierrez. 2018. A Radiative Transfer Framework for Spatially-Correlated Materials. *ACM Trans. Graph.* 37, 4 (2018).

Edward W Larsen. 2007. A generalized Boltzmann equation for non-classical particle transport. In *Proceedings of the International Conference on Mathematics and Computations and Supercomputing in Nuclear Applications*.

Edward W Larsen and Richard Vasques. 2011. A generalized linear Boltzmann equation for non-classical particle transport. *Journal of Quantitative Spectroscopy and Radiative Transfer* 112, 4 (2011).

Michael L Larsen and Aaron S Clark. 2014. On the link between particle size and deviations from the Beer–Lambert–Bouguer law for direct transmission. *Journal of Quantitative Spectroscopy and Radiative Transfer* 133 (2014), 646–651.

Jorge Lopez-Moreno, David Miraut, Gabriel Cirio, and Miguel A. Otaduy. 2015. Sparse GPU Voxelization of Yarn-Level Cloth. *Computer Graphics Forum* 36, 1 (2015).

George Marsaglia and Wai Wan Tsang. 2000. A simple method for generating gamma variables. *ACM Transactions on Mathematical Software (TOMS)* 26, 3 (2000), 363–372.

Johannes Meng, Marios Papas, Ralf Habel, Carsten Dachsbacher, Steve Marschner, Markus Gross, and Wojciech Jarosz. 2015. Multi-Scale Modeling and Rendering of Granular Materials. *ACM Trans. Graph.* 34, 4 (2015).

Raymond A Shaw, Alexander B Kostinski, and Daniel D Lanterman. 2002. Super-exponential extinction of radiation in a negatively correlated random medium. *Journal of quantitative spectroscopy and radiative transfer* 75, 1 (2002), 13–20.
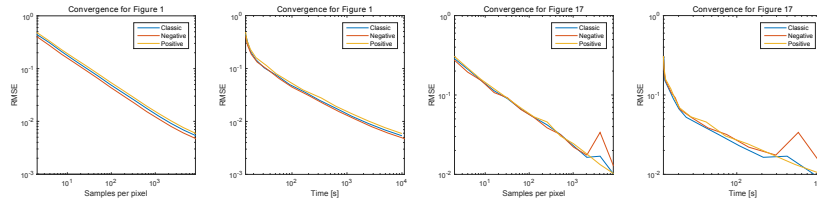
Fig. S.6. Convergence plots for the scenes in Figures 1 and 17, relating the RMSE with the number of samples and rendering time, respectively. Each scene is rendered with different types of media: a classic exponential medium, a negatively correlated medium, and a positively correlated medium modeled with our model in Section 5.2.

Fig. S.7. Convergence series for increasing number of samples (from left to right: 2, 8, 64, 128, 512 samples per pixel) on the scene shown in Figure 1 for different types of media. From top to bottom: negatively correlated media, classic exponential media, and positively correlated media.
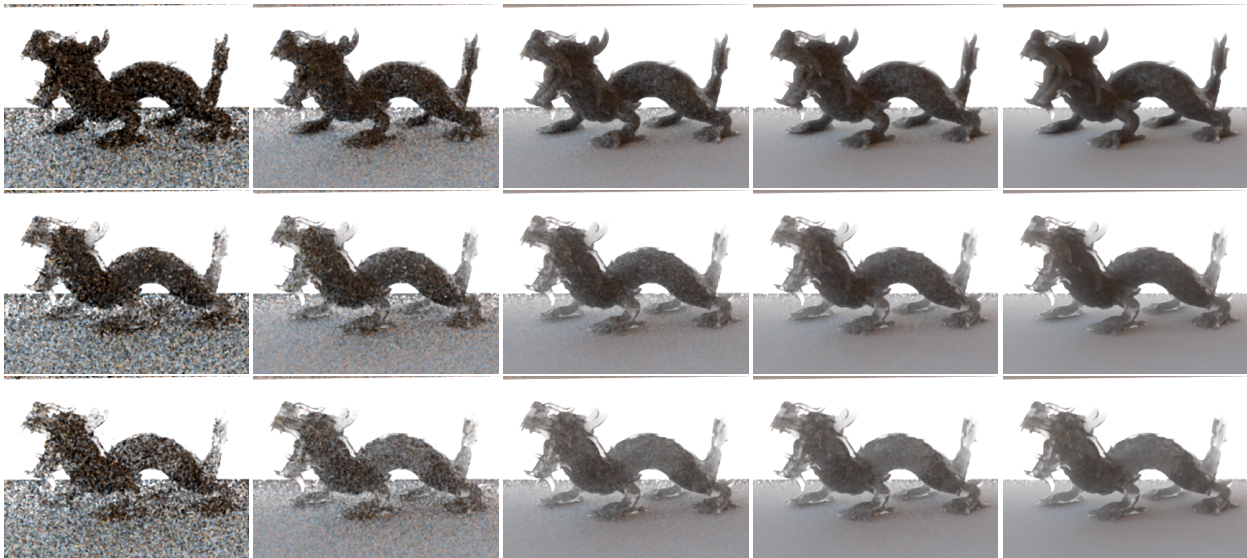
Fig. S.8. Convergence series for increasing number of samples (from left to right: 2, 8, 64, 128, 512 samples per pixel) on the scene shown in Figure 17 for different types of media. From top to bottom: negatively correlated media, classic exponential media, and positively correlated media.
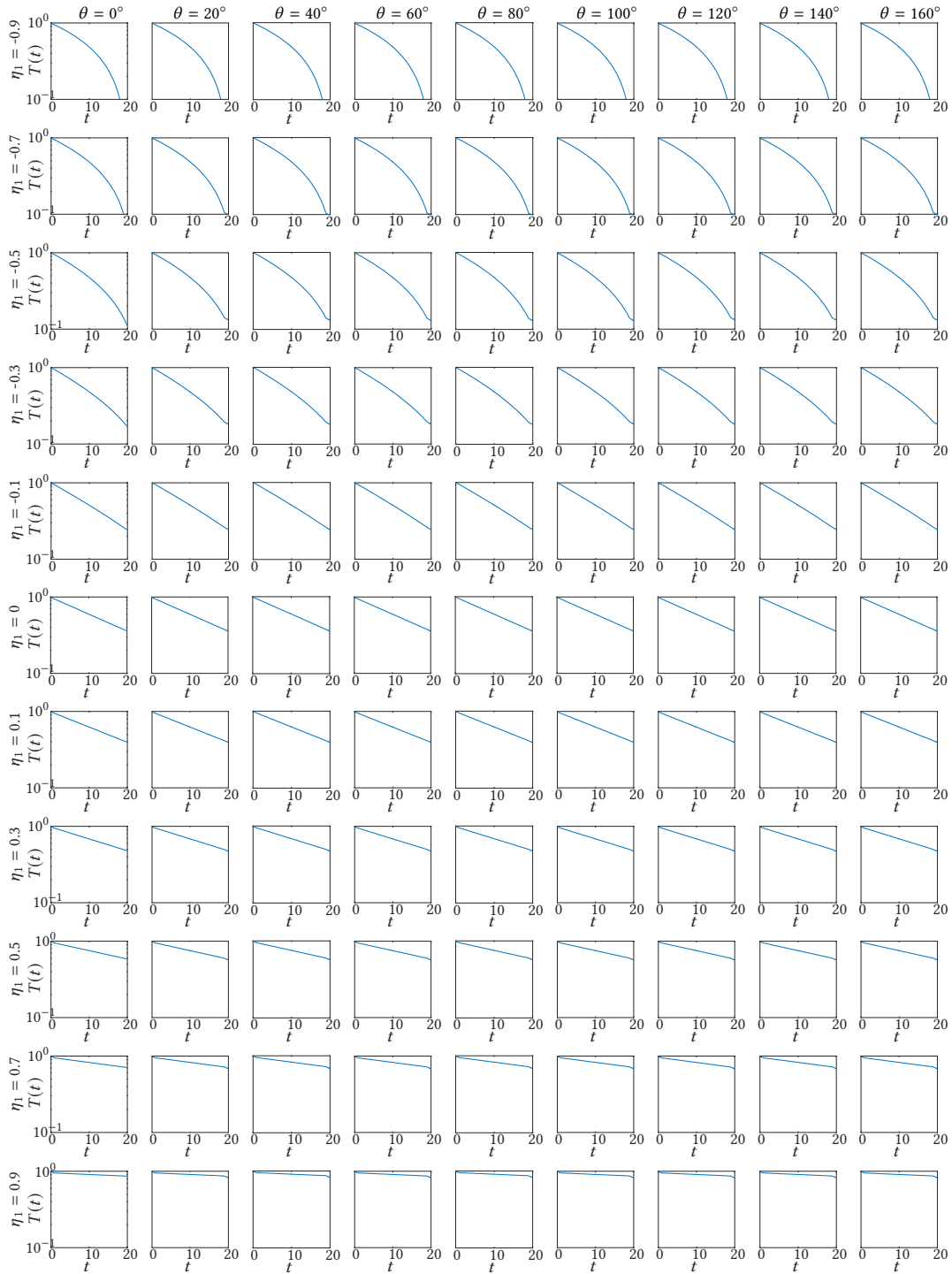
Fig. S.9. Monte Carlo simulations of the transmittance $T_Q(t)$ from rays with origin at sources, for infinite media with correlation varying from $\eta_1 \in [-1, 0.9]$, in logarithmic scale, for different angles θ.
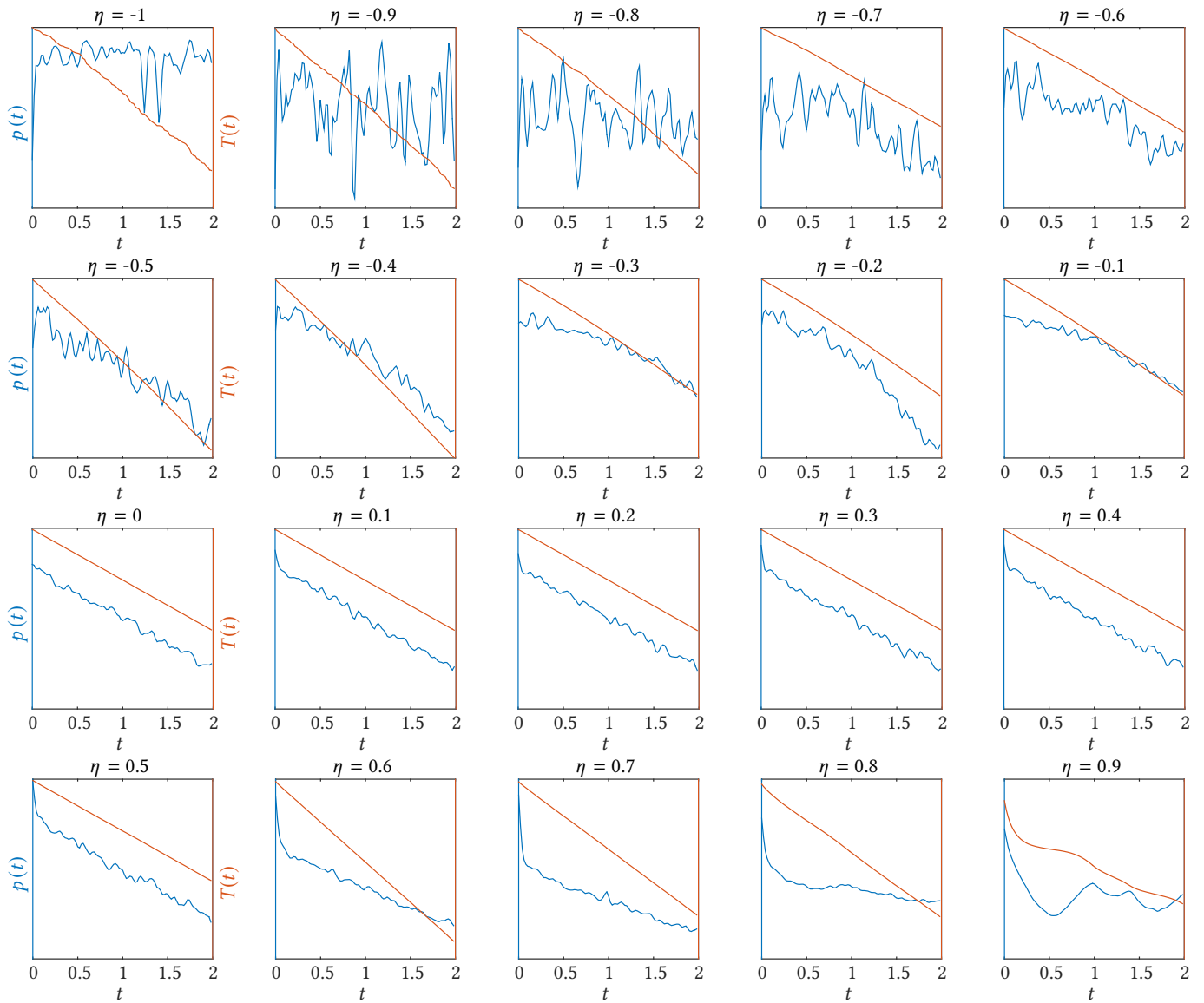
Fig. S.10. Monte Carlo simulations of the probability distribution of extinction $p_S(t)$ (blue) and transmittance $T_S(t)$ (orange) from rays with origin at scatterers, for infinite media with correlation varying from $\eta_1 \in [-1, 0.9]$, in logarithmic scale.
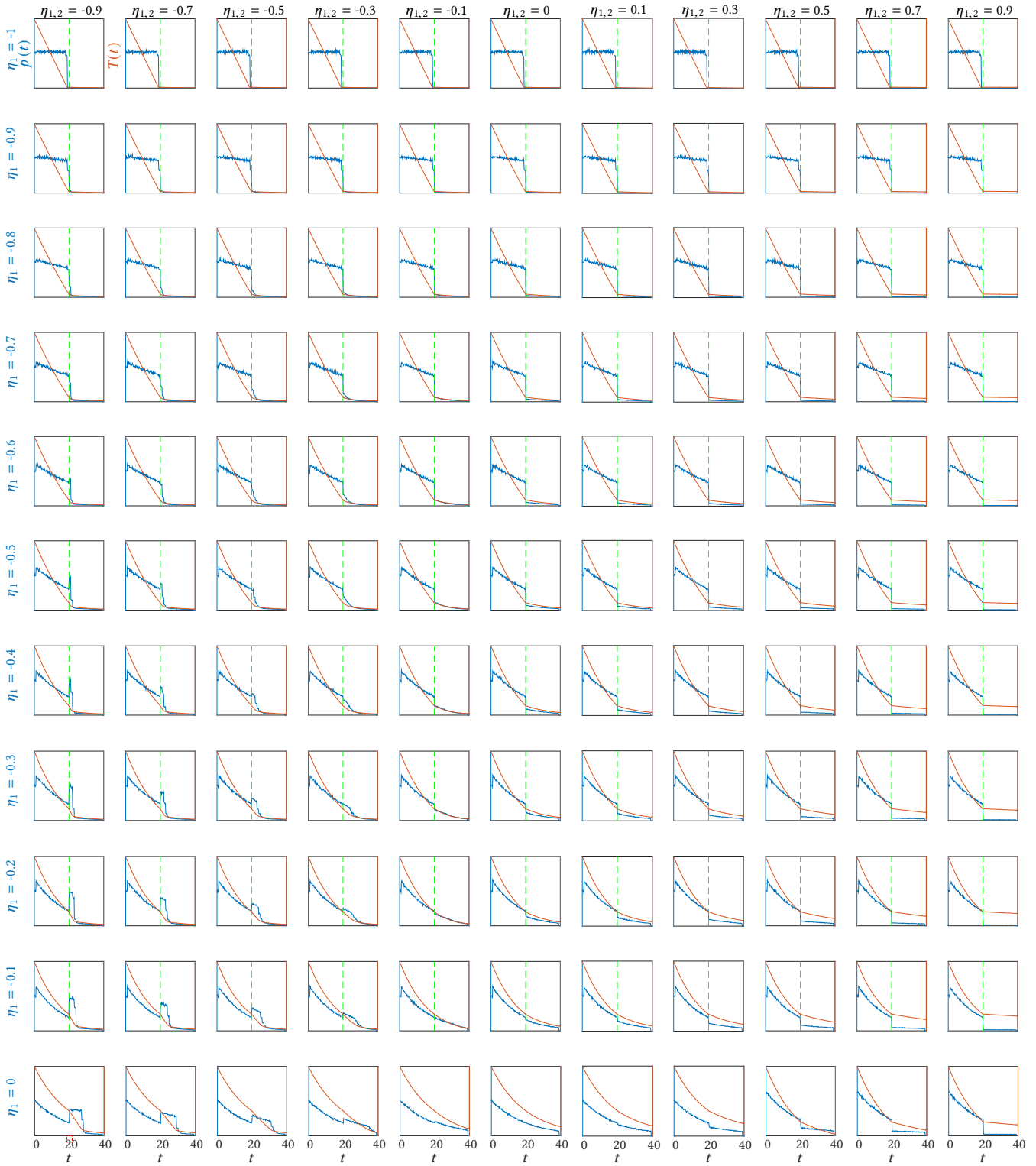
Fig. S.11. Monte Carlo simulations for the medium-to-medium boundary (marked as a green dashed line), showing the probability distribution of extinction $p(t)$ (blue), and transmittance $T_Q(t)$ (orange), for original media with correlation $\eta_1 \in [-0.9, 0]$, and second media defined so that the correlation between both media $\eta_{1,2} \in [-0.9, 0.9]$ infinite media with correlation varying from $\eta_1 \in [-1, 0.9]$.
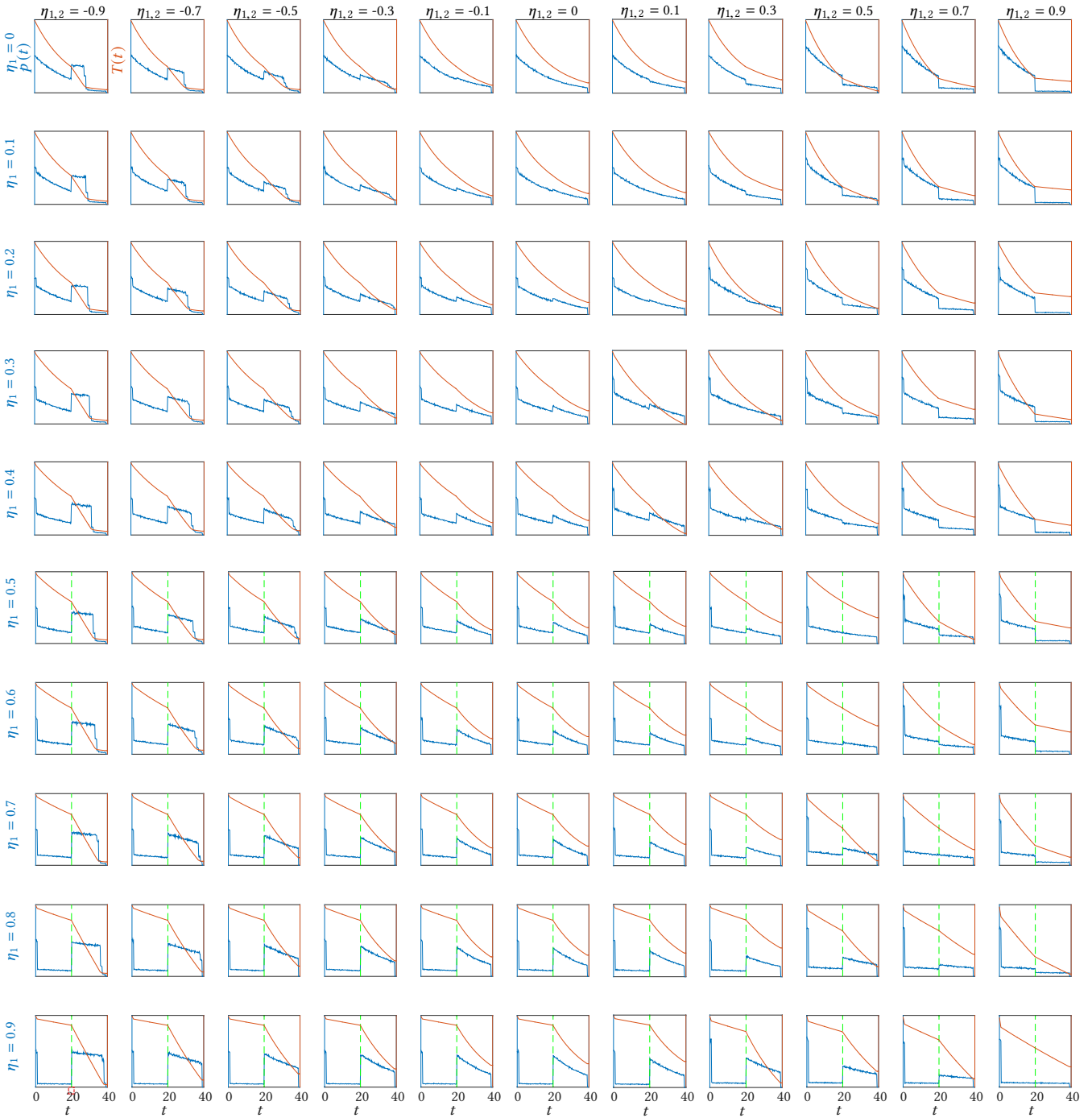
Fig. S.12. Monte Carlo simulations for the medium-to-medium boundary (marked as a green dashed line), showing the probability distribution of extinction $p(t)$ (blue), and transmittance $T_Q(t)$ (orange), for original media with correlation $\eta_1 \in [0, 0.9]$, and second media defined so that the correlation between both media $\eta_{1,2} \in [-0.9, 0.9]$ infinite media with correlation varying from $\eta_1 \in [-1, 0.9]$.
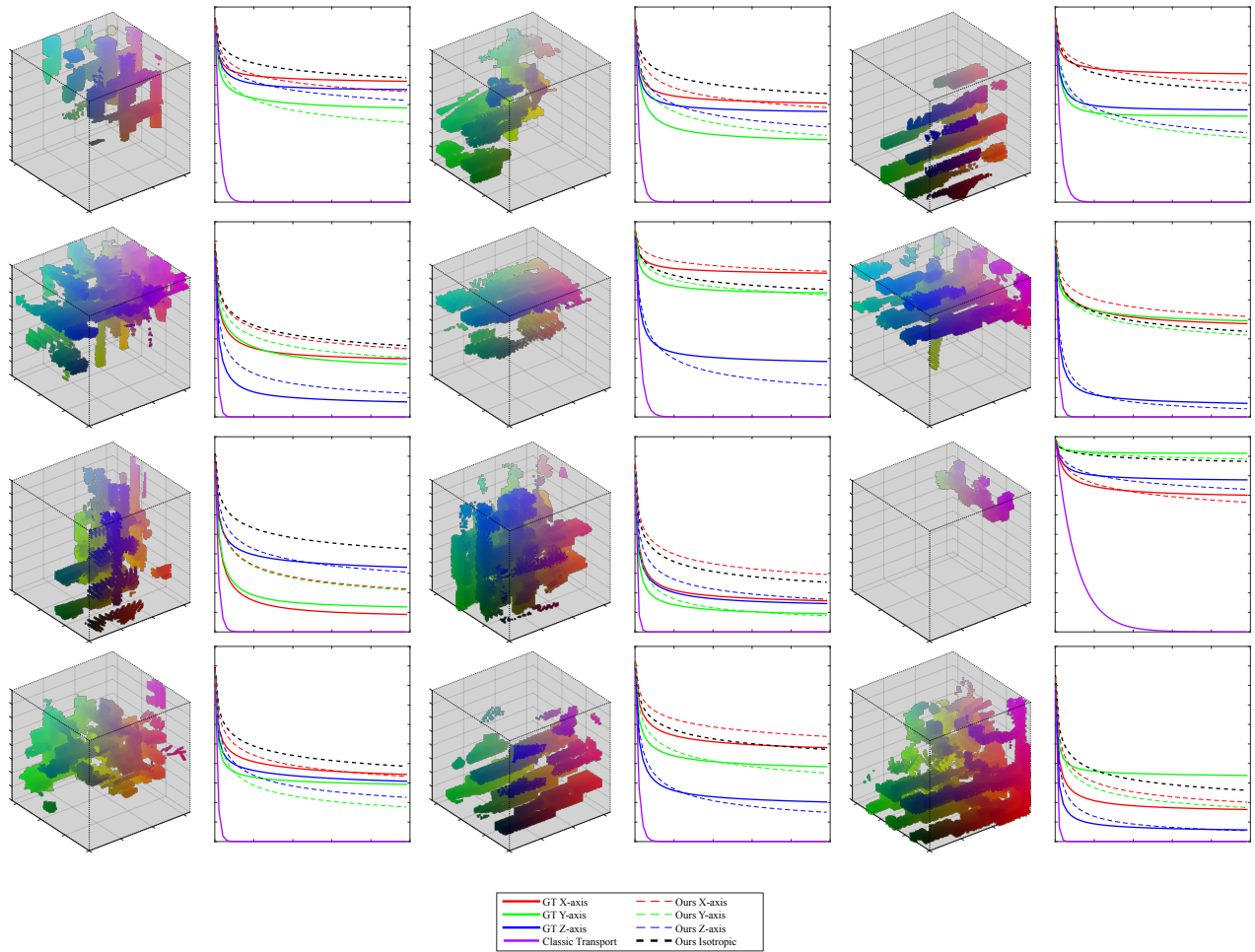
Fig. S.13. Additional examples of transmittance in high-resolution volumes of locally-correlated media (procedurally generated after [Lopez-Moreno et al. 2015]). Beams of light travel through each volume, aligned in succession to the x, y, and z axes. Ground truth transmittance (red, green, and blue solid lines) has been computed by brute force regular tracking [Amanatides and Woo 1987], while our simulation (dotted lines) uses the gamma distribution proposed in Equation 19. Classic transport governed by the RTE significantly overestimates extinction through the volume, resulting in a exponential decay (purple line). In contrast, our model matches ground-truth transmission much more closely. The black dotted line is the result of isotropic correlation, which is clearly also non-exponential.